

# The Coulomb Blockade in Quantum Boxes

Eran Lebanon,<sup>1</sup> Avraham Schiller,<sup>1</sup> and Frithjof B. Anders<sup>2</sup>

<sup>1</sup>Racah Institute of Physics, The Hebrew University, Jerusalem 91904, Israel

<sup>2</sup>Institut für Festkörperphysik, TU Darmstadt, 64289 Darmstadt, Germany

The charging of a quantum box connected to a lead by a single-mode point contact is solved for arbitrary temperatures, tunneling amplitudes, and gate voltages, using a variant of Wilson's numerical renormalization group. The charge inside the box and the capacitance of the junction are calculated on equal footing for all physical regimes, including weak tunneling, near perfect transmission, and the crossover regime in between. At the charge plateaus, perturbation theory is found to break down at fairly small tunneling amplitudes. Near perfect transmission, we confirm Matveev's scenario for the smearing of the Coulomb-blockade staircase. A surprising reentrance of the Coulomb-blockade staircase is found for large tunneling amplitudes. At the degeneracy points, we obtain two-channel Kondo behavior directly from the Coulomb-blockade Hamiltonian, without the restriction to two charge configurations or the introduction of an effective cutoff.

PACS numbers: 73.23.Hk, 72.15.Qm, 73.40.Gk

The Coulomb blockade<sup>1,2</sup> is one of the fundamental phenomena in mesoscopic physics. When a quantum box, either a small metallic grain or a large semiconducting quantum dot, is coupled by weak tunneling to a lead, its charging is governed by the finite energy barrier  $E_C$  for adding a single electron to the box. This gives rise to the well-known Coulomb-blockade staircase for the charge of the box as a function of gate voltage.<sup>1,2</sup> Increasing the coupling to the lead smears the Coulomb staircase, as thermal fluctuations do at  $k_B T > E_C$ .

A large diversity of theoretical approaches have been applied to the Coulomb blockade, ranging from perturbation theory<sup>3,4,5,6</sup> and diagrammatic techniques,<sup>7,8,9</sup> to renormalization-group treatments<sup>4,5,10,11,12</sup> and Monte Carlo simulations.<sup>11,12,13,14</sup> However, to date there is no single unified approach encompassing all regimes of the Coulomb blockade. The reason being that different starting points are required for describing the different physical regimes of the Coulomb blockade. For weak tunneling and  $k_B T \ll E_C$ , the charge inside the box is essentially quantized at the charge plateaus. Hence, one can start from a well-defined charge configuration and apply the perturbation theory in the tunneling amplitude. This approach collapses at the degeneracy points between adjacent charge plateaus, where strong charge fluctuations give rise to exotic many-body physics in the form of the two-channel Kondo effect.<sup>5,15</sup> For large transmission, the Coulomb-blockade staircase is smeared out and the notion of well-defined charge configurations breaks down.

In this paper, we devise such a unified approach for all temperatures and parameter regimes of the Coulomb blockade using Wilson's numerical renormalization-group method.<sup>16</sup> Focusing on single-mode point contacts, we accurately calculate the charge and the capacitance of the quantum box, for arbitrary gate voltages, temperatures, and tunneling amplitudes. These quantities were recently measured by Bernan et al. for single-mode point contacts,<sup>17</sup> revealing signatures of the two-channel Kondo effect. For weak tunneling, we recover the results of the perturbation theory at the charge plateaus. However, we

find that the perturbation theory breaks down at fairly small tunneling amplitudes. Close to perfect transmission, we find good agreement with Matveev's analysis of a related model,<sup>18</sup> which in turn breaks down as one departs from perfect transmission. Upon further increasing the tunneling matrix element, there is a surprising reentrance of the Coulomb-blockade staircase. At the degeneracy points, we obtain two-channel Kondo behavior directly from the Coulomb-blockade Hamiltonian, without the restriction to two charge configurations or the introduction of an effective cutoff. Indeed, the effective cutoff entering Matveev's two-charge-configuration model<sup>1</sup> is found to depend not only on the charging energy  $E_C$ , but also on the tunneling strength.

The coupled quantum-box-lead system is conventionally modeled by the Hamiltonian

$$H = \sum_{\mathbf{k}} \sum_{\sigma} \epsilon_{\mathbf{k}} c_{\mathbf{k}\sigma}^\dagger c_{\mathbf{k}\sigma} + \frac{\hat{Q}_B^2}{2C_0} + V_B \hat{Q}_B + t \sum_{\mathbf{k}} c_{L\mathbf{k}}^\dagger c_{B\mathbf{k}} + H_L + H_B; \quad (1)$$

where  $c_{L\mathbf{k}}^\dagger$  ( $c_{B\mathbf{k}}^\dagger$ ) creates a lead (box) electron with momentum  $\mathbf{k}$  and spin  $\sigma$ ;  $t$  is the tunneling matrix element, taken for simplicity to be momentum independent; and  $\epsilon_{L\mathbf{k}}$  ( $\epsilon_{B\mathbf{k}}$ ) are the single-particle levels in the lead (box), which are assumed to be continuous (dense energy levels). The excess electrical charge inside the box,

$$\hat{Q}_B = e \sum_{\mathbf{k}} [c_{B\mathbf{k}}^\dagger c_{B\mathbf{k}} - (c_{B\mathbf{k}}^\dagger + c_{B\mathbf{k}})] \quad (2)$$

( $e$  being the electron charge), is controlled by the capacitance of the box,  $C_0$ , and by the external component of the electrostatic potential in the box,  $V_B$ .

The numerical renormalization group<sup>16</sup> (NRG) is a nonperturbative approach for treating quantum impurity problems. At the center of this approach is a logarithmic energy discretization of the conduction band around

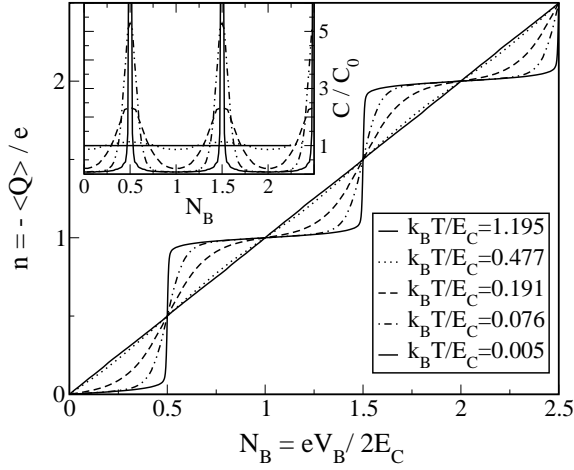


FIG. 1: The excess charge inside the box versus  $V_B$ , for  $t = 0.1$  and different temperatures. Here,  $E_C = D = 0.01$ ,  $\epsilon = 2.5$ , and  $N_s = 2000$ . At temperatures comparable to the charging energy, the charge curve is essentially linear. A sharp Coulomb-blockade staircase emerges for  $k_B T \ll E_C$ . Inset: The capacitance versus  $V_B$ , for the same temperatures as plotted in the main panel. For  $k_B T \gg E_C$ , the capacitance is constant and equal to  $C_0 = e^2/2E_C$ . For  $k_B T \ll E_C$ , sharp capacitance peaks develop at the degeneracy points.

the Fermi level, designed to capture all logarithmic divergences of the problem. Using a unitary transformation, the conduction band is mapped onto a semi-infinite chain with the impurity coupled to the open end, and a hopping matrix element that decreases exponentially along the chain. A direct application of this approach to the Coulomb-blockade Hamiltonian is doomed to fail, since the Coulomb interaction equally couples all sites along the semi-infinite chain. It does not decay as the hopping matrix elements. To circumvent this problem, we resort to a mapping used by Schoeller and co-workers.<sup>7,10</sup> Explicitly, we map the Hamiltonian of Eq. (1) onto

$$H = \sum_{k,k'} \sum_n \sum_{l,m} t_{lk} c_{lk}^\dagger c_{lk} + \frac{\hat{Q}^2}{2C_0} + V_B \hat{Q} + t \sum_{k,k'} \hat{Q} c_{lk}^\dagger c_{lk} + H_{\text{sc}}; \quad (3)$$

where

$$\hat{Q} = \sum_n j_n \quad \text{and} \quad \hat{Q} = \sum_n e_n j_n \quad (4)$$

are new collective charge operators. Strictly speaking, the above mapping requires the constraint  $\hat{Q} = \hat{Q}_B$ . However, this constraint can be relaxed in the continuum limit, when the dynamics of  $\hat{Q}$  in Eq. (3) is insensitive to the precise number of conduction electrons in the bands. Hereafter, we regard  $\hat{Q}$  as an independent degree of freedom.

Equation (3) describes two noninteracting conduction bands, coupled to an impurity with an infinite number

of parabolically dispersed energy levels. Hence, it can be treated using the NRG. We solved this model using a common constant density of states for the lead and the box,<sup>19</sup> and a common bandwidth  $D$ . The NRG method is controlled by the logarithmic discretization parameter and by the number of states retained  $N_s$ .<sup>16</sup>

Figure 1 shows the expected Coulomb-blockade staircase at different temperatures, for the weak tunneling  $t = 0.1$ . At temperatures above the charging energy  $E_C = e^2/(2C_0)$ , one recovers a linear (classical) charge curve. As the temperature is reduced below the charging energy, a staircase structure emerges, with a period equal to twice the charging energy. For  $k_B T \ll E_C$ , one is left with sharp charge steps, with abrupt transitions between the charge plateaus at half-integer values of  $N_B = eV_B/2E_C$ .

A complementary picture is provided by the capacitance,  $C = d\langle Q \rangle/dV_B$ , recently measured by Bernan et al.<sup>17</sup> As seen in the inset of Fig. 1, the capacitance  $C$  is equal to the classical capacitance  $C_0$ , for  $k_B T \gg E_C$ . However,  $C$  acquires a strong dependence on  $N_B$ , for  $k_B T \ll E_C$ . While  $C$  is significantly reduced at the charge plateaus, near the degeneracy points (i.e., near half-integer values of  $N_B$ ) it is dramatically enhanced. As will be discussed below,  $C$  diverges logarithmically at the degeneracy points as  $T \rightarrow 0$ , in accordance with the two-channel Kondo effect predicted by Maltsev.<sup>5</sup>

At the charge plateaus, perturbation theory in  $t$  is commonly used for weak tunneling. To second order in  $t$ , the zero-temperature excess number of electrons inside the box,  $n = \langle Q \rangle/e$ , is given by

$$n = 2(t)^2 \ln \frac{1 + 2N_B}{1 - 2N_B} + 2 \ln \frac{1 - 2N_B + d}{1 + 2N_B + d} + \ln \frac{1 + 2N_B + 2d}{1 - 2N_B + 2d}; \quad (5)$$

Here, we have considered particle-hole symmetric bands, and retained a finite ratio  $d = D/E_C$ . In the wide-band limit,  $d \rightarrow 1$ , the last two terms drop in Eq. (5), and one recovers the conventional expression (see, e.g., Ref. 6).

The inset of Fig. 2 compares between the NRG and the perturbative expression of Eq. (5). At very weak tunneling,  $t = 0.05$  and  $0.1$ , the NRG results coincide with the perturbative expression. The good agreement extends to all gate voltages except the vicinity of the degeneracy points. However, significant deviations from Eq. (5) are seen at fairly weak coupling,  $t = 0.2 - 0.3$ . Indeed, the Coulomb-blockade staircase is completely washed out for  $t = 0.3$  (main panel of Fig. 2), indicating the breakdown of the perturbation theory. Moreover, there is a reentrance of the Coulomb-blockade staircase for  $t > 0.4$ , which obviously is not captured by the perturbation theory in  $t$ .

The rapid breakdown of the perturbation theory is related to the approach to perfect transmission. For  $E_C = 0$  and particle-hole symmetric bands, the single-particle transmission coefficient at the Fermi level is given

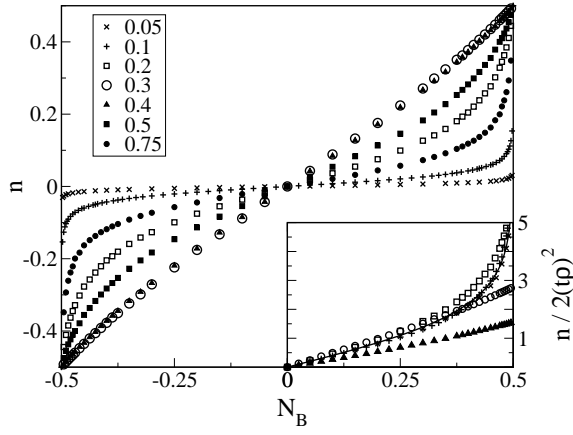


FIG. 2: Evolution of the zero-temperature charging curve with increasing  $t$ . Here,  $E_C = D = 0.01$ ,  $\gamma = 2.5$ , and  $N_s = 2000$ . The values of  $t$  are specified in the legend. At very weak coupling, there is a sharp Coulomb-blockade staircase. As demonstrated in the inset, good agreement is obtained with the perturbative expression for  $n = 2(t)^2$  [see Eq. (5)], which is plotted for comparison by the solid line. Significant deviations from the perturbation theory develop for  $t > 0.2$ . Specially, the Coulomb-blockade staircase is completely washed out for  $t = 0.3$ , marking the breakdown of the perturbation theory. For  $t > 0.4$ , there is a reentrance of the Coulomb-blockade staircase.

by

$$T = 4 \frac{(t)^2}{[1 + (t)^2]^2} : \quad (6)$$

For  $t = 1$ ,  $T$  reaches perfect transmission and is no longer perturbative in  $t$ . That  $T$  rather than  $t$  is the relevant physical parameter for  $E_C = D$  is evident from Fig. 2. The Coulomb-blockade staircase is washed out for  $t = 0.3 - 0.4$ , when  $T$  of Eq. (6) approaches unity. The reentrance of the Coulomb-blockade staircase for  $t > 0.4$  stems from the reduction of the single-particle transmission coefficient with increasing  $t > 1$ . It should be emphasized, however, that this picture is only valid for  $E_C = D$ . Upon increasing  $E_C$ , the charge curves cannot be exclusively parametrized by the transmission coefficient of Eq. (6). In particular, the washing out of the Coulomb-blockade staircase and its subsequent reentrance are pushed to higher values of  $t$ , reflecting the limitations of the single-particle picture.

Near perfect transmission, it was predicted by Matveev that the zero-temperature excess number of electrons inside the box is given by<sup>18</sup>

$$n = N_B + \frac{2}{\pi} \frac{j^2}{j^2} \ln e^{j^2} \cos^2(N_B) \sin(2N_B) : \quad (7)$$

Here,  $j^2 = 1/T$  is the reactance, is equal to  $E_C$ , and  $C = 0.5772$  is Euler's constant. This result was obtained within a one-dimensional model, especially designed for  $T = 1$ . This regime of large transmission was never studied using a tunneling Hamiltonian.

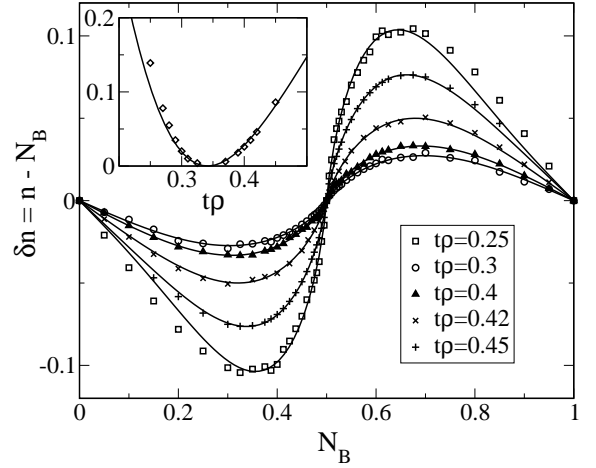


FIG. 3: Comparison of the NRG (symbols) and Eq. (7), for the zero-temperature charge curve near perfect transmission. Here,  $E_C = D = 0.01$ ,  $\gamma = 2.5$ , and  $N_s = 2000$ . The horizontal axis,  $n = n - N_B$ , measures the deviation from linearity of the excess number of electrons inside the box. The solid lines are fits to Eq. (7), using the single fitting parameter  $j^2$ . Inset: A plot of the extracted values of  $j^2$  versus  $t$ . The solid line shows  $1 - T$  of Eq. (6) with  $t \rightarrow t - 0.023$ .

Figure 3 shows a comparison of our NRG results for  $n = n - N_B$  and Eq. (7), using the single fitting parameter  $j^2$ . There is a good agreement between the two curves, particularly for  $0.3 \leq t \leq 0.4$ . Moreover, the extracted values of  $j^2$  closely trace  $1 - T$  in this range of  $t$  (see inset of Fig. 3), apart from a slight shift which is likely due to the finite value of  $E_C = D$  used. For  $t = 0.25$  and  $t = 0.45$ , small systematic deviations from Eq. (7) develop in the middle of the plateaus, near integer values of  $N_B$ . Further away from perfect transmission, e.g., for  $t = 0.2$  and  $t = 0.5$  (not shown), there are large deviations from the analytic expression, signaling the breakdown of Matveev's expression. This clearly shows that one can still use the tunneling Hamiltonian of Eq. (1) near perfect transmission, provided that the tunneling processes are summed to all orders.

Of particular interest is the behavior near the degeneracy points, where the perturbation theory diverges logarithmically even for small values of  $t$ . For weak tunneling and  $k_B T \ll E_C$ , the charge fluctuations in this regime were mapped by Matveev<sup>5</sup> onto the planar two-channel Kondo model, by retaining only the two lowest-lying charge configurations inside the box. The capacitance at the degeneracy points was predicted to diverge logarithmically with  $T \rightarrow 0$ , in accordance with the logarithmic divergence of the magnetic susceptibility in the two-channel Kondo effect.<sup>15</sup> This scenario was never confirmed directly for the Hamiltonian of Eq. (1).

Figure 4 shows the capacitance at the degeneracy points as a function of temperature. At low temperatures, the capacitance diverges logarithmically with decreasing  $T$ , confirming the onset of the two-channel Kondo effect. Indeed, the two-channel Kondo effect per-

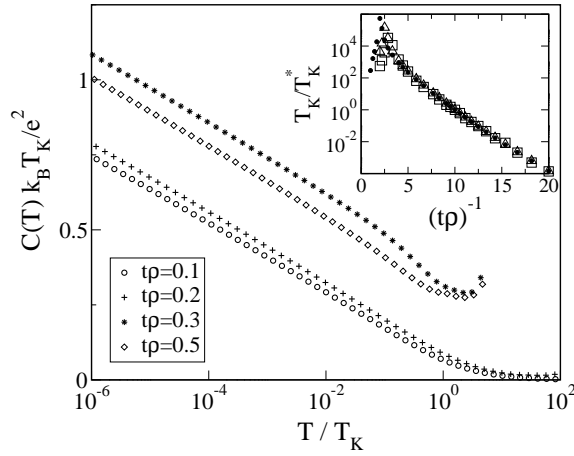


FIG. 4: The capacitance at the degeneracy points as a function of temperature, for  $E_C = D = 0.25$  and different values of  $t$ . Here,  $\gamma = 2$  and  $N_s = 2000$ . All curves show the characteristic logarithmic temperature dependence of the two-channel Kondo effect. Using Eq. (8), we extract the Kondo temperature  $T_K$  from the slope of the logarithmically diverging component of  $C(T)$ . Inset:  $T_K = T_K$  versus  $(t)^{-1}$ , for  $E_C = D = 0.01$  (open squares),  $0.25$  (open triangles), and  $1$  (dots). Here,  $T_K$  is the Kondo temperature for  $t = 0.1$ . Explicitly,  $k_B T_K = D$  equals  $3.2 \cdot 10^6$ ,  $3.6 \cdot 10^5$ , and  $6.5 \cdot 10^5$ , for  $E_C = D = 0.01$ ,  $0.25$ , and  $1$ , respectively.

sists for all values of  $E_C = D$  and all values of  $t$  up to perfect transmission, where it breaks down.<sup>18</sup> However, the logarithmic behavior is regained upon further increasing  $t$ , marking the reentrance of the two-channel Kondo effect.

The crossover from the high-temperature to the low-temperature universal regime is generally marked by the Kondo temperature  $T_K$ , which we extract from the Bethe ansatz expression for the slope of the logarithmically diverging term in the capacitance:<sup>20</sup>

$$C(T) \sim \frac{e^2}{20k_B T_K} \ln(T_K = T) : \quad (8)$$

Within the two-charge-conjugation model of Matveev,  $T_K$  is given by<sup>5</sup>

$$T_K = D_e t \exp \left( -\frac{1}{4t} \right) ; \quad (9)$$

where  $D_e$  is an effective high-energy cutoff, assumed to be of the order of the charging energy.

In the inset of Fig. 4, we plotted  $T_K = T_K$  versus  $(t)^{-1}$ , for a wide range of charging energies  $E_C = D$ . Here,  $T_K$  is the Kondo temperature for  $t = 0.1$ , extracted separately for each value of  $E_C = D$ . For weak tunneling,  $T_K$  decays exponentially with  $(t)^{-1}$ , in accordance with Eq. (9). In particular, all curves fall on top of one another in this regime, confirming that  $E_C$  enters the expression for  $T_K$  only through the preexponential factor  $D_e$ . However, a detailed comparison of the NRG data and Eq. (9) reveals an additional dependence of  $D_e$  on  $t$ . For  $E_C = D = 0.01$ , for example,  $D_e$  is enhanced by a factor of 4 upon going from  $t = 0.05$  to  $t = 0.2$ . At perfect transmission, the two-channel Kondo effect breaks down, which is signaled by a cusp in  $T_K$  as a function of  $t$  [the slope of the  $\ln(T)$  component of  $C(T)$  vanishes]. In contrast to the universality of the weak-tunneling regime, the position of the cusp in  $T_K$  shifts to higher values of  $t$  with increasing  $E_C$ , showing that one cannot exclusively parameterize the system by the noninteracting transmission coefficient of Eq. (6).

In summary, we devised an NRG approach for solving the charging of a quantum box connected to a lead by a single-mode point contact, which uniformly treats all regimes of the Coulomb blockade. Using this approach we are able to (i) reveal the rapid breakdown of the perturbation theory, (ii) obtain a surprising reentrance of the Coulomb-blockade staircase for large tunneling amplitudes, (iii) confirm Matveev's scenario for the shape of the charge curve near perfect transmission, and (iv) obtain two-channel Kondo behavior at the degeneracy points directly from the Hamiltonian of Eq. (1).

E.L. and A.S. were supported in part by the Centers of Excellence Program of the Israel Science Foundation, founded by The Israel Academy of Science and Humanities. F.B.A. was supported in part by DFG grant No. AN 275/2-1.

<sup>1</sup> D.V. Averin and K.K. Likharev, in *Mesoscopic Phenomena in Solids*, edited by B.A. Altshuler, P.A. Lee, and R.A. Webb (Elsevier, Amsterdam, 1991).

<sup>2</sup> *Single Charge Tunneling*, Vol. 294 of NATO Advanced Studies Institute, Series B: Physics, edited by H. Grabert and M.H. Devoret (Plenum Press, New York, 1992).

<sup>3</sup> G. Schon and A. Zaikin, *Phys. Rep.* **198**, 237 (1990).

<sup>4</sup> L.I. Glazman and K.A. Matveev, *Zh. Eksp. Teor. Fiz.* **98**, 1834 (1990) [*Sov. Phys. JETP* **71**, 1031 (1990)]; *Phys. Ma*

*Zh. Eksp. Teor. Fiz.* **51**, 425 (1990) [*JETP Lett.* **51**, 484 (1990)].

<sup>5</sup> K.A. Matveev, *Zh. Eksp. Teor. Fiz.* **99**, 1598 (1991) [*Sov. Phys. JETP* **72**, 892 (1991)].

<sup>6</sup> H. Grabert, *Phys. Rev. B* **50**, 17364 (1994); G. Goppert, H. Grabert, N.V. Prokof'ev, and B.V. Svistunov, *Phys. Rev. Lett.* **81**, 2324 (1998).

<sup>7</sup> H. Schoeller and G. Schon, *Phys. Rev. B* **50**, 18436 (1994).

<sup>8</sup> D.S. Golubev and A.D. Zaikin, *Phys. Rev. B* **50**, 8736

- (1994).
- <sup>9</sup> E. Lebanon, A. Schiller, and V. Zevin, Phys. Rev. B 64, 245338 (2001).
  - <sup>10</sup> J. König and H. Schoeller, Phys. Rev. Lett. 81, 3511 (1998).
  - <sup>11</sup> G. Falki, G. Schon, and G. T. Zimanyi, Phys. Rev. Lett. 74, 3257 (1995).
  - <sup>12</sup> W. Hofstetter and W. Zwerger, Phys. Rev. Lett. 78, 3737 (1997).
  - <sup>13</sup> X. Wang, R. Egger, and H. Grabert, Europhys. Lett. 38, 545 (1997).
  - <sup>14</sup> C. P. Herrero, G. Schon, and A. D. Zaikin, Phys. Rev. B 59, 5728 (1999).
  - <sup>15</sup> For a review of the multichannel Kondo effect, see D. L. Cox and A. Zawadowski, Adv. Phys. 47, 599 (1998).
  - <sup>16</sup> K. G. Wilson, Rev. Mod. Phys. 47, 773 (1975).
  - <sup>17</sup> D. Berman, N. B. Zhitenev, R. C. Ashoori, and M. Shayegan, Phys. Rev. Lett. 82, 161 (1999).
  - <sup>18</sup> K. A. Matveev, Phys. Rev. B 51, 1743 (1995).
  - <sup>19</sup> Actually, is the geometric average of the density of states in the lead and in the box.
  - <sup>20</sup> P. D. Sacramento and P. Schlottmann, Phys. Lett. A 142, 245 (1989).